New Activated Carbon from Wormwood as Efficient Adsorbent of Cationic Dye in Aqueous Solution

Akhrib, Kenza*[+]; Bensmaili, Aicha; Bouafia-Chergui, Souad
Reaction Engineering Laboratory, Faculty of Process Engineering and Mechanical Engineering, University of Science and Technology Houari Boumediene, BP 32, Bab Ezzouar, 16111, Algiers, ALGERIA

Kadmi, Yassine
Université de Lille, LASIR; UMR CNRS 8516, Villeneuve d'Ascq, FRANCE

ABSTRACT: *This investigation deals with the potential use of new activated carbon as an adsorbent. This later was prepared from wormwood residues consisting of Artemisia vulgaris pharmaceutic plant by-product. This carbon was characterized using a Scanning Electron Microscopy(SEM) and Fourier Transform InfraRed (FT-IR) techniques before and after treatment with phosphoric acid. Batch adsorption experiments were conducted to study the adsorbent effectiveness in removing a cationic dye, basic yellow 28, from an aqueous solution. The effects of adsorbent dosage, dye concentration and initial pH on the elimination of the dye were analyzed. The results show that the equilibrium data were correctly represented using the Langmuir adsorption isotherm. The adsorption capacity of activated carbon toward the cationic dye was 357.14 mg/g obtained at 20°C. The kinetic study indicates that the adsorption process of dye on activated carbon follows a pseudo-second-order equation. The efficiency of this process was tested for real effluent; the adsorbent was able to reduce the concentration of total organic carbon.*

KEYWORDS: *Adsorption; Activated carbon; Isotherm; Elimination; Environment*

INTRODUCTION

Wastewater from textile, paper and some other industries contains residual dyes, which are not readily biodegradable. Adsorption and chemical coagulation are two common techniques used to treat such wastewater. The presence of synthetic dyes in wastewater could destroy the natural quality of the aquatic environment and also cause detrimental long-term health and environmental effects [1, 2]. Since these dyes are generally recalcitrant, biodegradation is not instantaneous due to the complexity of their aromatic molecular structures. Thus, these synthetic dyes can not be completely degraded by conventional treatment processes [3-6].

The removal of color from dyestuff manufacturing industry wastewater represents a major environmental concern. The strongest impact of this kind of wastewater on the environment is related to primary water consumption (80–100 m^3/ton of finished textile) and wastewater discharge (115–175 kg of chemical oxygen demand [COD]/ton of finished textile), organic chemicals, color and salinity [7].

**To whom correspondence should be addressed.*
+E-mail: *a_kenze@yahoo.fr*

1021-9986/2020/6/137-148 12/$/6.02

Recently, natural inorganic and agricultural adsorbents have attained significant appeal [8-11]. Alternative adsorbents, including wood sawdust [12], agroindustrial waste [13], zeolite [14], bentonite [15], peat [16], clays [17], fish waste [18], pistachio nutshells [19] and ash [20], have gained the interest of researchers in the dye removal field. Compared with conventional processes, the adsorption processes for wastewater treatment possess numerous advantages, such as low initial investment requirement, simplicity of implantation, no toxicity of resulting compounds and superior efficiency [21-24].

The main objective of the present study is to investigate the efficiency of a new Activated Carbon (AC) derived from agricultural waste Wormwood for the removal of BY28, as cationic dye, from aqueous solutions. Characterization of AC was performed using Scanning Electron Microscopy (SEM)and Fourier Transform InfraRed (FT-IR) techniques. For this purpose, various influence parameters namely the adsorbent dosage, the initial dye concentration and the solution pH were examined. The equilibrium data were tested with the Langmuir and Freundlich isotherm models. Also, different kinetic models for the adsorption of dye were presented. In order to investigate the efficiency of the prepared AC, the adsorption of real tannery effluent solution was finally studied.

EXPERIMENTAL SECTION

Preparation of activated carbon

The residues of a pharmaceutic plant (wormwood) were washed with distilled water to remove unwanted residues, crushed and dried at 100°C for 24 hours to reduce the moisture content. The obtained product is called the precursor. In order to increase its surface area and porosity, this precursor was impregnated with a chemical reagent (H_3PO_4). Afterwards, the precursor was carbonized in a muffle furnace at 600°C for 1.5 h. The carbonaceous residue was then washed with distilled water and heated at 100°C for 24 hours in an oven. The resulting product consisting of the AC was used in our experiments. AC characterization was achieved using (1) Fourier Transform InfraRed (FT-IR) for surface morphology analysis, (2) point of zero charge measurements, (3) SEM for determining porosity and morphological structure, and (4) Brunauer-Emmett-Teller (BET) to measure the surface area.

Adsorbate

BY28, provided by Textile Algerian Company (Textile Processing Industry of Bab-Ezzouar, Algiers, Algeria), was used without any purification. Its chemical structure and other characteristics are listed in Table 1. A stock solution of 200 mg/L was prepared by dissolving the required amount of BY28 dye in distilled water. The pH of the solution was adjusted to the desired value using 1.0 M HCl or NaOH solutions.

Real effluent

Supplied by the Textile Algerian Company, the real effluent contains not only BY28 dye, but also other dyes, chemical substances and auxiliaries used in the dyeing process. The different characteristics of the real effluent after dilution and the results of the adsorption test are presented in Table 7. The COD of the textile effluent before COD_0 and after COD_f adsorption was measured by an automated COD analyzer. The conductivity, the pH and the turbidity of the real effluent were measured using a conductimeter (Consort 861 K), pH-meter (Hanna pH 211) and turbidity-meter (Merck Turbiquant 1500T) respectively. Otherwise, the TOC measurement allowed determining the mineralization efficiency of the process. TOC values were determined by catalytic oxidation using a Shimadzu VCSH TOC analyzer. Before the adsorption, the real effluent was centrifuged (3000 rpm, 30 min) to remove the suspended solids. Thereafter, the liquid was diluted 10 times because of the high COD (1632 mg/L). The conductivity and the pH of the solution were 2.3 mS/cm and 5.21 respectively.

Adsorption studies and analytical method

The adsorption processes of AC in the aqueous solutions of BY28 were carried out using different operating parameters, after which the equilibrium concentrations were determined at the maximum absorbance wavelength of 400 nm. The sorption capacity q_t(in mg/g) at any time t was obtained as follows:

$$q_t = (C_0 - C_t).\frac{v}{m} \tag{1}$$

C_0 and C_t (mg/L) are, respectively, the liquid-phase concentrations of solutes initially and at a given time *t*, *v* (L) is the solution volume and m is the mass of the catalyst (g).

The amount of adsorption at equilibrium, q_e, is given by:

Table 1:Characteristics of BY28 dye.

Characteristics of BY28 dye					
Name	CI	Type	λ_{max}(nm)	M ($g.mol^{-1}$)	Chemical structure
Sandocryl Gold yellow B-GRL 300%	Basic Yellow 28	Cationic	440	433	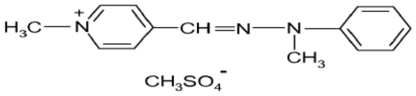

Table 2: Textural characteristics of the activated carbon.

Sample	SN_2 (m^2/g)	V_{Poreux} (cm·g)	Iodine number (mg/g)	pH_{pzc}	Bulk density	Humidity (%)
AC	1584	0.19	925	4.1	0.609	8.62

$$q_e = (C_0 - C_e).\frac{v}{m} \qquad (2)$$

C_e (mg/L) is the BY28 concentration at equilibrium.

The decrease in the concentration of cationic dye BY28 was followed via its characteristic absorption wavelength at 440 nm using a UV–visible spectrophotometer (UV-SOFAS-MONACO). Most of the experiments were performed in triplicate, and the arithmetic average is given. The percentage removal (R%) of BY28 is determined from the relation:

$$R\% = \frac{C_0 - C_t}{C_0} * 100 \qquad (3)$$

C_t (mg/L) is the concentration of BY 28 at the time (t).

RESULTS AND DISCUSSION

Characterization of AC adsorbent

To study the texture characterization of AC, the nitrogen surface area was obtained by applying the BET method to the N_2 adsorption isotherms at -196°C. The values for SN_2, the pore volume V_{Pore} and pH_{zero} are depicted in Table 2.

Scanning electron micrographs realized on raw (NDS), carbonized plant and AC at 600°C for 1.5 h are shown in Fig. 1. The SEM micrographs of carbonized precursor (carbonized plant) and AC are illustrated in Fig. 1a and 1b, respectively. SEM has been used as the primary tool for characterizing the surface morphology. Examination of the carbonization revealed a gradual porosity (Fig. 1a). This porosity grew more after activation for 2 h (Fig. 1b). A comparison of Figs. 1a and 1b indicates clearly that a regular porosity and a rather homogeneous surface are obtained by activation and carbonization at 600°C for 1.5 h. The morphology of AC attests to the substantial changes generated by H_3PO_4, and the adsorbent surface clearly shows a porous nature with a predominant microporous character, which are responsible for the increased surface area.

The EDX analysis (Fig. 1a) indicates that AC has high phosphorus content. This is due to both precursor chemical composition and the activating agent (H_3PO_4). Both parameters promote depolymerization, dehydration and redistribution of constituent biopolymers, inducing important changes in the pyrolytic decomposition of the lignocellulosic material.

The FT-IR spectra of AC, carbonized plant and AC after sorption in the range of 4000- 400 cm^{-1} are presented in Fig. 2 (a and c). The spectra show many absorption bands that are specific to the various functional groups. The strong band at 3444 cm^{-1} reflects the OH-stretching vibrations of carboxylic acids groups on the surface of AC, while the band at 2924 cm^{-1} corresponds to the CH stretch [25-26]. The distinct band at 1624 cm^{-1} was the result of the stretching vibration of C=O. The absorption bands at 1100 cm^{-1} and 1110 cm^{-1} are the characteristic peaks of symmetric and asymmetric C–O groups, respectively. The band at 1622 cm^{-1} could be attributed to the stretching vibration of C=C [27]. The same peaks are noted in the spectra of the treated plant, carbonized plant and treated plant after sorption, as shown in Fig. 2a (a-c). These results confirm that the structure of the plant is preserved after treatment. The pH_{pzc} indicates the acidic or basic character of the carbon surface. The combined influence of all functional groups of AC allows determining pH_{pzc}. This latter consists in the pH at which the net surface charge on carbon is zero [28]. The pH_{pzc} was determined by the method described by *Valliammai* [29]. The initial and final pH values after 48 h contact time with AC solutions (0.1 g per 25 mL) were measured.

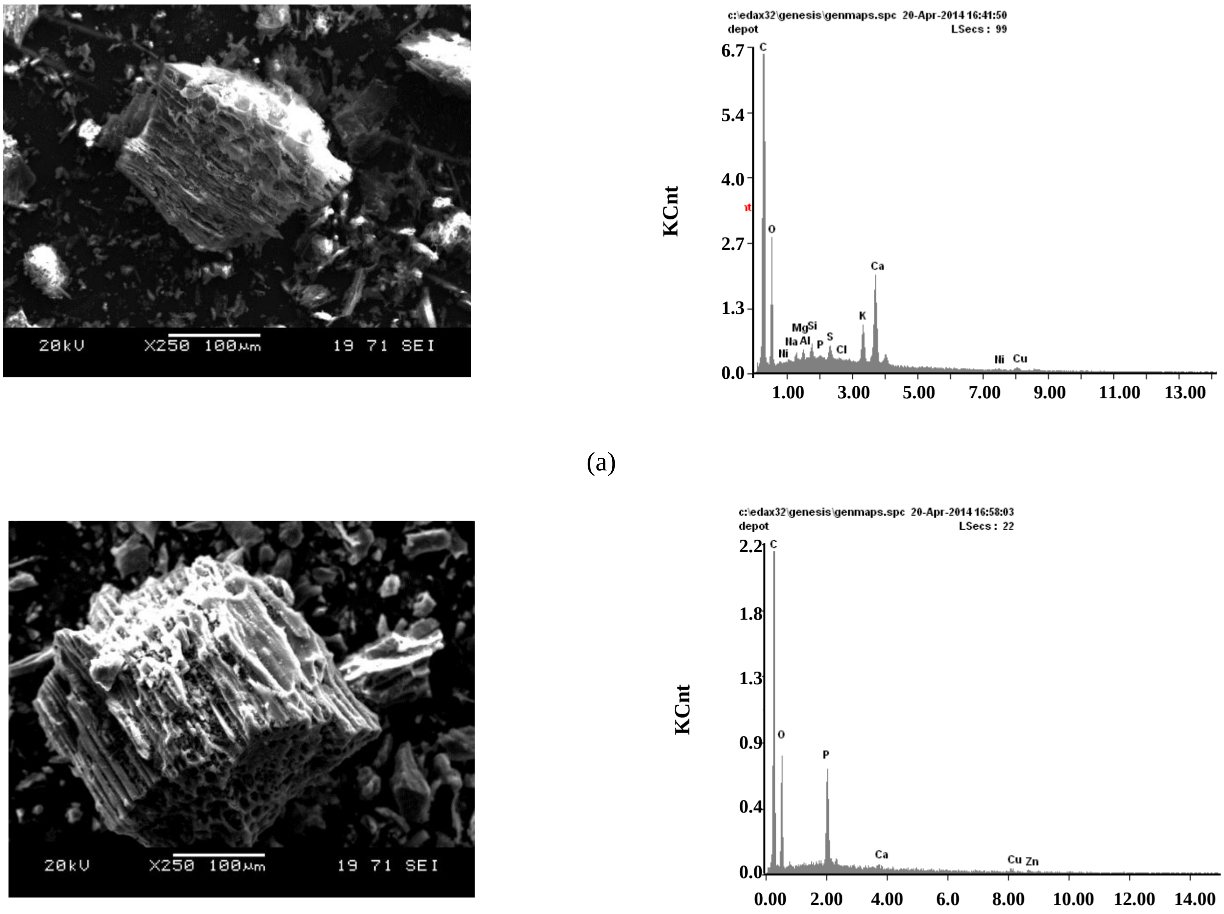

(a)

(b)

Fig. 1: SEM picture and EDX microanalysis of : (a) carbonized precursor and (b) activated plant.

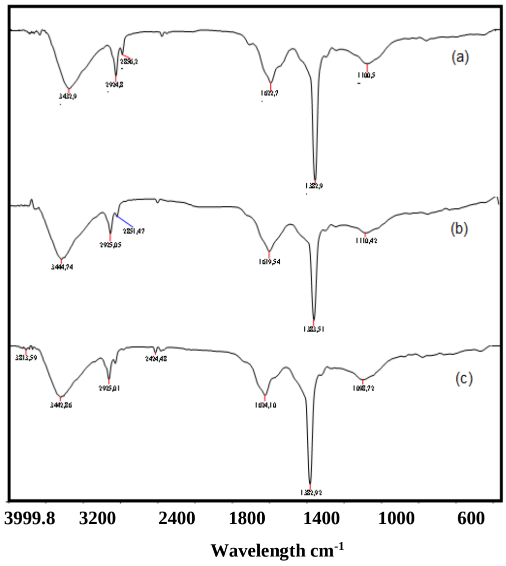

Fig. 2: FTIR spectra of AC (a), carbonized precursor (b), AC after sorption (c).

The pH_{pzc} corresponds to the point at which the initial and final pH values are equal. Experimental results revealed that the pH_{pzc} of the dye is 4.1.

Effect of experimental parameters on adsorption

Effect of adsorbent dose

To examine the effect of AC dose on BY28 adsorption, different concentrations of AC (varying from 0.25 to 1.5 g/L) were added to 100 mg/L BY28 solution; the other parameters consisting in $pH_{natural}$(without any pH adjustment) and stirring rate 400 rpm were kept constant. The effect of adsorbent dose on BY28 adsorption is shown in Fig. 3. With increasing the adsorbent dose, the BY28 removal rate increases from 30.94 to 99.65 % due to the increased availability of active sites of AC for the dye adsorption. For AC concentrations more than 1 g/L, the removal rate remains practically constant.

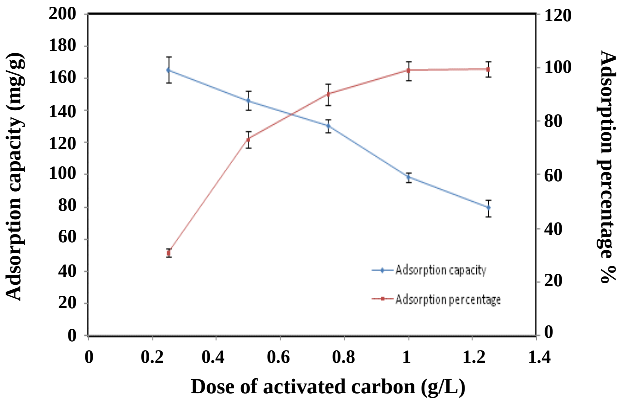

Fig. 3: The effect of adsorbent dose on the removal adsorption of BY28.

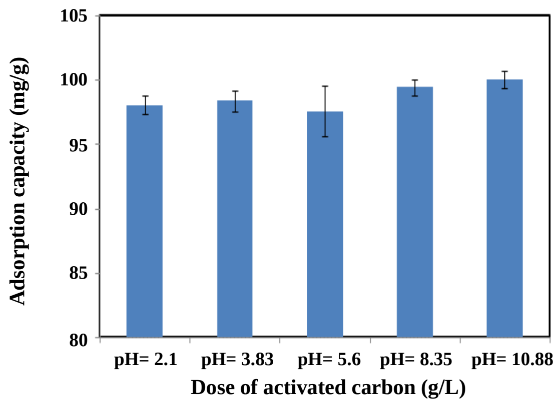

Fig. 4: The effect of initial pH of dye solution on adsorption capacity of the BY28.

Otherwise, the increase in adsorbent dose from 0.25 to 1.25 g/L leads to the adsorption capacity decreases from 165.28 to 79.56 mg/g. This may be attributed to the decrease in total adsorption surface area available to dye ions resulting from overlappingor aggregation of adsorption sites. Similar observations have been previously reported by some researchers [28]. For further adsorption experiments, AC dose of 1 g/L was chosen to study the influence of the dye concentration.

Effect of pH

The pH of an aqueous solution has been reported as having a significant influence on the adsorptive uptake of dye molecules due to its impact on both the surface binding sites of the adsorbent and the ionization process of the dye molecule [28]. For this purpose, the BY28 adsorption has been measured at initial pH values in the range of 2 to 10.8. In fact, the pH values were adjusted by drop-wise addition of 0.1 M HCl and 0.1 M NaOH solutions. The absorbent initial concentration, the shaking time, the temperature and the amount of adsorbent were fixed at 100 mg/L, 120 min, 20°C and 1 g, respectively. The results are presented in Fig. 4. This later reveals that pH has a very slight effect on the removal efficiency of the dye, indicating a high amount of acidic group’s on the exterior surface of AC. A similar observation is reported by Regti et al., 2016 for the BY28 removal from aqueous solution by activated carbon from medlar species.

Effect of initial dye concentration

The initial concentration provides an important driving force to overcome the mass transfer resistance of all of the molecules between the aqueous and solid phases [30]. To examine the effect of initial BY28 concentration, 1L solution of initial dosages of 40, 50, 75 and 100 mg/L were agitated with 1 g of AC at $pH_{naturel}$. The corresponding results giving the BY28 absorbance as function of contact time are depicted in Fig. 5.

From this figure, the BY28 adsorption increases abruptly during the initial period of contact time and slightly elsewhere before reaching the adsorption equilibrium. The rapid adsorption at the contact time beginning can be attributed to the availability of active sites on the surface. The low rate increase of adsorption is probably due to the slow pore diffusion of the adsorbate molecule into the bulk of the adsorbent [31].

In the adsorption process, dye molecules first encounter the boundary layer film, diffuse then onto the adsorbent surface and finally diffuse into the AC porous structure [30]. However, the adsorbed amount of BY28 was smaller at lower initial concentrations and greater at higher initial ones. It was also seen that an increase in initial concentrations resulted in increased dye uptake.

As shown in Fig. 5, the required time to reach equilibrium is 40 min, which was selected as the contact time for further experiments. The adsorption capacity at equilibrium (q_e) increased from 39.68 to 97.55 mg/g with an increase in the initial BY28 concentration from 40 to 100 mg/L. This may be attributed to the increase in the driving force of the concentration gradient resulting from the increase in the initial concentration of adsorbate [31].

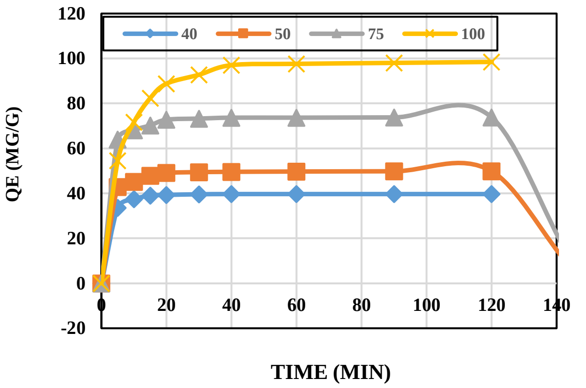

Fig. 5: Effect of initial dye concentration on the adsorption of BY28.

Adsorption kinetic

To investigate adsorption kinetics, pseudo-first-order and pseudo-second-order models using experimental data have been developed. The best fit model has been selected according to the linear regression correlation coefficient (R^2) values.

The pseudo-first-order kinetic model can be given as [32,33]:

$$\frac{dq}{dt} = k_1 \left(q_e - q_t \right) \quad (3)$$

Where k_1(min^{-1}) is the constant rate of adsorption, and q_t and q_e are the adsorbed amounts at a given time t and at equilibrium (mg/g), respectively.

After integration between 0 and a given time t, the model becomes [34]:

$$\ln\left(\frac{qe - qt}{qe} \right) = -k_1.t \quad (4)$$

The pseudo-second-order model kinetic equation is [33,35]:

$$\frac{dq}{dt} = k_2.\left(q_e - q_t \right)^2 \quad (5)$$

where k_2 is the rate constant of the pseudo-second-order equation (g/mg/min).

Integration leads to:

$$\frac{t}{q_t} = \frac{t}{k_2.q_e{}^2} + \frac{t}{q_e} \quad (6)$$

The linearized method was used to determine the parameters of the kinetic models. These parameters were calculated from the slope and intercept of their respective plots. Table 3 lists the results of the kinetic parameters of models at different BY22 concentrations.

For all studied parameters, the correlation coefficients for the first-order model are relatively lower than those obtained for the second-order kinetic model for the various pH, the initial BY28 concentrations and the AC doses.

The good agreement between the experimental and the calculated values of the maximum adsorption capacitiesstands in favor of the second-order kinetic model (Table 4). Indeed, the second-order kinetic model can be correctly applied to predict BY28 adsorption onto AC.

Because the pseudo-first-order and pseudo-second-order kinetic models cannot identify the diffusion mechanism, the kinetic results were then analyzed using the intra-particle diffusion model. The mechanism of the adsorption process is usually demonstrated by four steps: (i) bulk diffusion; (ii) film diffusion; (iii) pore diffusion or intra-particle diffusion; and (iv) adsorption of adsorbate on the adsorbent surface. The rate-controlling steps mainly depend on either surface or pore diffusion [28]. The Weber and Morris model given by Eq. (7) is widely used in intra-particle diffusion to predict the rate-controlling step [36,37]:

$$q_t = k_p.t^{\frac{1}{2}} \quad (7)$$

Note that kinetic parameters of the above-mentioned model are already given in Table 3.

Fig. 6 shows the plot of intra-particle diffusion of BY28 onto AC. According to the obtained results, it could be concluded that the intra-particle diffusion model shows a good fit, indicating that diffusion of dye into the pores of adsorbents has a significant influence on the adsorption mechanism. The data showed two linear evolutions. The first one consists in a linear increase, while the second is represented by a constant level. The first linear trend is due to the intra-particle diffusion of adsorbate through the solution. The constant level corresponds to the equilibrium stage. It is due to the low adsorbate concentration remaining in the solution.

In fact, the slope of the first linear portion gives the intra-particle rate constant (kid), and the intercept of this portion is proportional to the thickness of the boundary layer [29]. The dependences q_t vs. $t^{1/2}$ are linear and do not pass through the origin. Therefore, intra-particle diffusion is not the rate-determining step, and boundary layer control may be involved in the adsorption process.

Table 3: Kinetic parameter values for dye adsorption of BY28 by activated carbon.

Kinetic model parameters		Concentration of BY28 (mg/L)			
		40	50	75	100
Pseudo-first-order	k_1	0.242	0.477	1.439	2.1
	R^2	0.9643	0.9469	0.9293	0.9801
Pseudo-second order	$k_2(10^3)$	13.5	24.2	21.1	3.1
	R^2	0.9698	0.9998	0.9999	0.9998
Pore diffusion	K_p	2.6114	2.8727	3.8383	15.451
	R^2	0.9946	0.9879	0.9946	0.9879

Table 4: Calculated values of the maximum adsorption capacities.

Kinetic model parameters		Concentration of BY28 (mg/L)			
		40	50	75	100
	$q_e$exp (mg/g)	40.65	50.25	74.07	101.01
Pseudo-first-order	$q_e$theo (mg/g)	26.57	33.07	46.40	82.92
Pseudo-second order	$q_e$theo (mg/g)	39.68	49.81	73.65	99.57

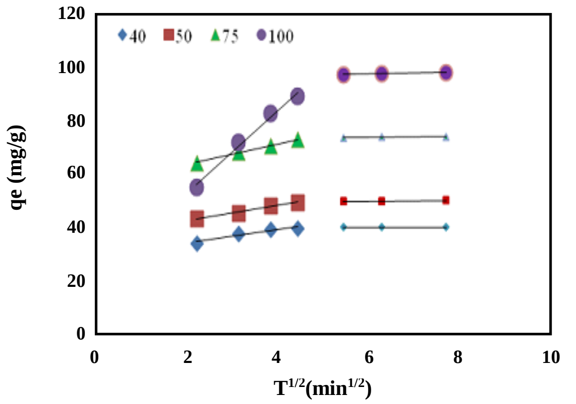

Fig. 6: Intra-particle diffusion plot for the removal of BY28.

The same results were also obtained by *Baccar* [38] for the adsorption of tannery dye on AC.

Adsorption isotherm

The interaction between adsorbate and adsorbent can be described by the adsorption isotherm. The shape of the isotherm is the first experimental tool used to diagnosethe nature of the adsorption phenomenon [28]. Two famous isotherm models of Langmuir and Freundlich were applied to the experimental data [39].

The Langmuir model assumes monolayer coverage of adsorbate on an energetically identical homogeneous adsorbent surface [40,41]. The Langmuir linearized form may be written as:

$$\frac{C_e}{q_e}=\frac{1}{b}+\frac{q_0}{b}.C_e \tag{8}$$

where b (L/mg) is the binding constant and q_0(mg/g) refers to the maximum adsorption capacity, evaluated by potting the C_e/q_e against C_e.

The Freundlich isotherm is derived by assuming a heterogeneous surface with a non-uniform distribution of heat of adsorption over the surface. The Freundlichadsorption isotherm equation and its linear form can be written as follows [42] :

$$Lnq_e = LnK_f + \frac{1}{n}\text{LnC} \tag{9}$$

Where K_f is a constant indicative of the relative adsorption capacity of the adsorbent, and n is a constant indicative of the intensity of the adsorption. Constants were obtained from the plot of log (q_e) versus log (C_e) that should give a straight line with a slope of (1/n) and an intercept of log (K_f). All data are depicted in Table 5. Comparing the regression coefficient values for both Langmuir and Freundlich isotherms, it was demonstrated that the Langmuir isotherm was the most appropriate to describe the equilibrium data, confirming the monolayer biosorption. Table 6 shows the comparison of

Table 5: Freundlich and Langmuir isotherm constants of adsorption of BY28 on AC.

Freundlich constants			Langmuir constants		
K_F	N	R^2	q_m(mg/g)	b (L/mg)	R^2
9.11	1.5	0.90	357.14	0.019	0.97

Table 6: Comparison of the maximum monolayer adsorption of BY28 onto various adsorbents.

Adsorbent	q_{max} (mg .g^{-1})	Adsorbate	References
AC(wormwood)	357.14	BY28	This study
coffee grounds	10	BY2	[43]
Activated sludge	56.98	BY24	[44]
Amberlite XAD-4	8.7–14.9	BY28	[45]
Clinoptilolite	52.9–59.6	BY28	[45]
GO	68.5	BY28	[46]
Boron waste	75.0	BY28	[47]
HMCN	909.1	BY28	[48]
AC (Ziziphusmauritiana nuts)	200	BY28	[49]
Bentonite	256.4	BY28	[50]
Boron industry waste	75	BY28	[47]
AC (wild olive stones)	118.2	BY28	[51]
Clinoptilolite	59.6	BY28	[45]
AC (Ziziphus lotus stone)	423.73	BY28	[52]
Kudzu	160	BY21	[53]
Peanut husk	96.2	yellow	[54]
Apricot stone	134.6	yellow 7	[55]

the maximum monolayer adsorption of BY28 onto various adsorbents.

Application to wastewater from the textile industry

Considering the effectiveness of the adsorption process for removal of BY28 dye, experiments were carried out to test its practical application for the mineralization of real wastewater from Textile Processing Industry of Bab-Ezzouar, Algiers (Algeria). This wastewater contains BY28 and a high concentration of organic matter. The adsorption experiment was performed in batch mode under AC optimal concentration of 1g/l, natural pH (without any adjustment), magnetic stirring (400 rpm, 3 h) and 20°Ctemperature. The different characteristics of the textile effluent before and after treatment are summarized in Table 7.

The results of the physical examination indicate a complete decolorization and a decrease in the turbidity level from 826 to 78 NTU. Chemical examination results show that the COD value decreased from 1632 mg/L to 192 mg/L and the TOC from 597 mg/L to 327 mg/L.

Table 7: Characteristics of the textile effluent before and after treatment.

	Turbidity (NTU)	pH	Conductivity(S/m)	TOC (mg/L)	COD (mg/L)
Real effluent	826	5.21	2.3	597.7	1632
Real effluent after adsorption onto AC	78	7.37	2.3	327.8	192

CONCLUSIONS

This study investigated the potential use of a new AC derived from wormwood (pharmaceutic plant) as adsorbent for the removal of BY28 from aqueous solution. AC was characterized by SEM, FTIR and BET. The effect of adsorbent dosage, dye concentration and pH were experimentally studied to evaluate the adsorption capacity, kinetics and isotherm. The results show that AC could be employed to remove cationic dye from aqueous solutions. The dye removal process obeys a pseudo- second-order kinetic expression. Adsorption of BY28 on AC follows the Langmuir isotherm. The results of treating the textile effluent with AC reveal a total decolorization and a decrease in turbidity, COD and TOC. Finally, the new AC has proved its effectiveness in the real effluent treatment field.

Received :Apr. 11, 2019 ; Accepted : Jul. 1, 2019

REFERENCES

[1] Forgacs E., Cserhati T., Oros G., Removal of Synthetic Dyes from Wastewaters: a Review, *Environ. Int.*, **30(7)**: 953-971 (2004).

[2] Vijayaraghavan G., Shanthakumar S., Effective Removal of Acid Black 1 Dye in Textile Effluent Using Alginate from Brown Algae as a Coagulant, *Iran. J. Chem. Chem. Eng. (IJCCE)*, **37(4)**: 145-151 (2018).

[3] Vatanpour V., Salehi E., Sahebjamee N., Ashrafi M., Novel Chitosan/Polyvinyl Alcohol thin Membrane Adsorbents Modified with Detonation Nanodiamonds: Preparation, Characterization, and Adsorption Performance, *Arabian Journal of Chemistry.*, (In press 2018).

[4] Sakin O.O., Ali Hussein M., Hussein H.M.B., Mgaidi A., Adsorption Thermodynamics of Cationic Dyes (methylene blue and crystal violet) To a Natural Clay Mineral From Aqueous Solution Between 293.15 and 323.15 K, *Arab. J. Chem.*, **11(5)**: 615-623 (2018).

[5] El-Gohary F., Tawfik A., Decolorization and COD Reduction of Disperse and Reactive Dyes Wastewater Using Chemical-Coagulation Followed by Sequential Batch Reactor (SBR) Process, *Desalination.*,**249(3)**: 1159-1164 (2009).

[6] Bouafia-Chergui S., Oturan N., Khalaf H., Oturan M. A., Parametric Study on the Effect of the Ratios $[H_2O_2]/[Fe^{3+}]$ and $[H_2O_2]$/[substrate] on the Photo-Fenton Degradation of Cationic Azo Dye Basic Blue 41, *J. Environ. Sci. Health.*,**45(5)**: 622-629 (2010).

[7] Savin I.I., Butnaru R., Wastewater Characteristics in Textile Finishing Mills, *Environ. Eng. Management Journal*, **6(7)**: 859-864(2008).

[8] Carmalin Sophia A., Eder C. Lima., Removal of Emerging Contaminants from the Environment by Adsorption, *Ecotoxicology and Environmental Safety.*, **150**:1-17 (2018).

[9] Crini G., Non-conventional Low-Cost Adsorbents for Dye Removal: AReview,*Bioresour, Technol.*,**97(9)**: 1061-1085 (2006).

[10]Robinson T., McMullan G., Marchant R., Nigam P., Remediation of Dyes in Textile Effluent. A Critical Review on Current Treatment Technologies with a Proposed Alternative, *Bioresour. Technol.*, **77(3)**: 247-255 (2001).

[11] Langeroodi N. S ., Safaei E., Carbonized Medlar-Core Particles as a New Biosorbent for Removal of Cu2þ from Aqueous Solution and Study of Its Surface Morphology, *Water. Science.and Technology.*, **74:(1)**: 236-245(2016).

[12] Garg V.K., Gupta R., Yadav A.B., Kumar R., Dye Removal from Aqueous Solution by Adsorption on Treated Sawdust, *Bioresour. Technol.*, **89(2)**: 121-124(2003).

[13] Kurniawan A., Kosasih A.N., Febrianto J., Ju Y.H., Sunarso J., Indraswati N., Ismadji S., Evaluation of Cassava Peel Waste as Lowcost Biosorbent for Nisorption: Equilibrium, Kinetics, Thermodynamics and Mechanism, *Chem. Eng. J.*, **172**: 158-166 (2011).

[14] Yousef R.I., El-Eswed B., Al-Muhtaseb A.H., Adsorption Characteristics of Natural Zeolites as Solid Adsorbents for Phenol Removal from Aqueous Solutions: Kinetics, Mechanism, and Thermodynamics Studies, *Chem. Eng. J.*,**171(3)**: 1143-1149 (2011).

[15] Volzonen C., Beatriz Garrido L., Use of Modified Hydroxy-Aluminum Bentonites for Chromium (III) Removal From Solution**s**, *J. Environ. Manage.*,**88(4)**: 1640-1648(2008).

[17] Espantaleón A.G., Nieto J.A., Fernández M., Marsal A., Use of Activated Clays in the Removal of Dyes and Surfactants From Tannery Wastewaters, *Appl. Clay. Sci.*,**24(1-2)**: 105-110 (2003).

[18] Dotto G.L., Pinto L.A.A., Adsorption of Food Dyes onto Chitosan: Optimization Process and Kinetic, *Carbohydr. Polym.*,**84(1)**: 231-238 (2011).

[19] Bazan-Wozniak A., Nowicki P., Pietrzak R., The Influence of Activation Procedure on the Physicochemical and Sorption Properties of Activated Carbons Prepared from Pistachio Nutshells for Removal of NO_2/H_2S Gases and Dyes, *J. Cleaner. Prod.*, **152**: 211-222 (2017).

[20] Mane V.S., Mall I.D., Srivastava V.C., Kinetic and Equilibrium Isotherm Studies for the Adsorptive Removal of Brilliant Green Dye from Aqueous Solution by Rice Husk Ash, *J. Environ. Manage.*, **84(4):** 390-400 (2007).

[21] Grainger S., Fu G.Y., Hall E.R., Biosorption of Colour-Imparting Substances in Biologically Treated Pulp Mill Effluent using Aspergillus Niger Fungal Biomass, *Water, Air, Soil Pollut.*,**217(1-4)**: 233-244 (2011).

[22] Noroozi B., Sorial G.A., Bahrami H., Arami M., Equilibrium and Kinetic Adsorption Studies of a Cationic Dye by a Natural Adsorbent-Silkworm Pupa, *J. Hazard. Mater.*,**139(1)**: 167-174 (2007).

[23] Elango G., Kumaran S.M., Kumar S.S., Muthuraja S., Roopan S.M., Green Synthesis of SnO_2 Nanoparticles and its Photocatalytic Activity of Phenol Sulfonphthhale in Dye, *Spectrochim Acta a Mol Biomol Spectrosc.*, **145**: 176-180 (2015).

[24] Vuono D., Catizzone E., Aloise A., Policicchio A., Agostino R.G., Migliori M., Giordano G., Modelling of Adsorption of Textile Dyes over Multi-walled Carbon Nanotubes: Equilibrium and Kinetic, *Chin. J. Chem. Eng.*,**25**: 523-532(2017).

[25] kaouah F., Boumaza S., Berrama T., Trari M., Bendjama Z., Preparation and Characterization of Activated Carbon from Wild Olive Cores (oleaster) by H_3PO_4 for the Removal of Basic Red 46, *Journal of Cleaner Production.*,**54**:296-306 (2013).

[26] Chee-Heong O., Wee-Keat C., Yoke-Leng S., Swee-Yong P., Fei-Yee Y., Conversion and Characterization of Activated Carbon Fiber Derived from Palm Empty Fruit Bunch Waste and its Kinetic Study on Urea Adsorption, *J. Environ. Manage.*,**197**: 199-205 (2017).

[27] Sun Y., Webley P.A., Preparation of Activated Carbons from Corncob with Large Specific Surface Area by a Variety of Chemical Activators and their Application in Gas Storage, *Chem. Eng.*,**162(3)**:883-892(2010).

[28] Güzel F., Sayğılı H., Akkaya S.G., Koyuncu, F., Decolorisation of Aqueous Crystal Violet Solution by a New Nanoporous Carbon: Equilibrium and Kinetic Approach, *J. Ind. Eng. Chem.*,**20(5)**: 3375-3386(2014a).

[29] Valliammai S., Subbareddy Y., Nagaraja K. S., Jeyaraj B., Adsorption of Erythrosine-B on Mesoporous Graphitic Activated Carbon Prepared from Bael Tree (Aeglemarmelos) Bark: Equilibrium, Kinetics and Thermodynamic Studies, *J. Mater. Environ. Sci.*,**6(10)**: 2836-2852(2015).

[30] Güzel F., Sayğılı H., Akkaya S.G., Koyuncu F., Elimination of Anionic Dye by Using Nanoporous Carbon Prepared from an Industrial Biowaste, *J. Mol. Liq.*,**194**: 130-140 (2014b).

[31] Sayğılı H ., Güzel F., Behavior of Mesoporous Activated Carbon used as a Remover in Congo Red Adsorption Process, *Water Sci Technol.*, **2017(1)**: 170-183 (2018).

[32] Lagergren S., About the Theory of so Called Adsorption of Soluble Substances, *Ksver. Veterskapsakad. Handl.*, **24**: 1-6 (1898).

[33] Ho Y.S., Mckay G., The Kinetics of Sorption of Divalent Metal Ions on Sphagnum Moss Peat, *Water Res.*,**34(3)**: 735-742 (2000).

[34] Al Abdullah J., Al Lafi A.G., Alnama T., Al Masri W., Amin Y., Adsorption Mechanism of Lead on Wood/Nano-Manganese Oxide Composite, *Iran. J. Chem. Chem. Eng. (IJCCE)*, **37(4)**:131-144 (2018).

[35] Ebrahimia M., Samadani Langeroodia N., Hooshmanda Sh., Biosorption of Fe(III) Ions Using Carrot: Equilibrium, Kinetics, and Statistical Analysis, *Protection of Metals and Physical Chemistry of Surfaces*, **55(2)**: 259-265 (2019)

[36] Weber W.J., Morris J.C., San J., Kinetics of Adsorption on Carbon from Solution, *Eng. Divis. Am. Soc. Civil. Eng.*, **89**: 31- (1963).

[37] Yang X., Al-Duri B., Kinetic Modeling of Liquid-Phase Adsorption of Reactive Dyes on Activated Carbon, *J. Colloid. Interface. Sci.*,**287(1)**: 25-34 (2005).

[38] Baccar R., Blánquez P., Bouzid J., Feki M., Sarrà M.,Equilibrium, Thermodynamic and Kinetic Studies on Adsorption of Commercial Dye by Activated Carbon Derived from Olive-Waste Cakes, *Chem. Eng. J.*,**165(2)**: 457-464(2010).

[39]ShahJ., Rasul JanM., MuhammadM.,Ara B.,Fahmeeda, Kinetic and Equilibrium Profile of the Adsorptive Removal of Acid Red 17 Dye by Surfactant-Modified Fuller's Earth, *Water Sci. Technol.*,**75(6)**: 1410–1420(2017).

[40] Regti A., Ben El Ayouchia H., Laamari M.R., Stiriba S., Anane H., El Haddad M., Experimental and Theoretical Study Using DFT Method for the Competitive Adsorption of two Cationic Dyes from Wastewaters, *Appl. Surf. Sci.*,**390**:311-319 (2016).

[41] HonorioJ.F.,Veit M.T., Gonçalves G.C.,Campos É.A., Fagundes-KlenM.R., Adsorption of Reactive Blue BF-5G Dye by Soybean Hulls: Kinetics, Equilibrium and Influencing Factors, *Water. Sci .Technol.*,**73**: 1166–1174(2015).

[42] Freundlich H.M.F., Uber Die Adsorption in Losungen, *Phys. Chem.*,**57** (A): 385-470 (1906).

Garg V.K., Gupta R., Yadav A.B., Kumar R., Dye Removal from Aqueous Solution by Adsorption on Treated Sawdust, *Bioresour. Technol.*, **89(2)**: 121-124(2003).

[43] Name A., Mekarziab A., Benrachedib K., Belhaneche-Bensemraa N., Hellala A., Determination of the Adsorption Capacity of Activated Carbon Made from Coffee Grounds by Chemical Activation with $ZnCl_2$ and H_3PO_4, *Journal of Hazardous Materials*.,**119(1-3)**: 189–194(2005).

[44] Chu H.C., Chen K.M., Reuse of Activated Sludge Biomass: II. The Rate Processes for the Adsorption of Basic Dyes on Biomass, *Process Biochemistry*, **37(10)**: 1129–1134 (2002)

[45]Yener J., Kopac T., Dogu G., Dogu T., Adsorption of Basic Yellow 28 from Aqueous Solutions with Clinoptilolite and Amberlite, *J. Colloid Interface Sci.*, **294(2)**: 255-264 (2006),

[46] Konicki W., Aleksandrzak M., Mijowska E., Equilibrium, Kinetic and Thermodynamic Studies on Adsorption of Cationic Dyes from Aqueous Solutions Using Graphene Oxide, *Chem. Eng. Res. Des.*, **123**:35-49(2017).

[47] Olgun A., Atar N., Equilibrium and Kinetic Adsorption Study of Basic Yellow 28 and Basic Red 46 by a Boron Industry Waste, *J. Hazard. Mater.*, **161(1)**: 148–156 (2009).

[48] Konicki W., Cendrowski K., Bazarko G., Mijowska E.,Study on Efficient Removal of Anionic, Cationic and Nonionic Dyes from Aqueous Solutions by Means of Mesoporous Carbon Nanospheres with Empty Cavity, *Chem. Eng. Res. Des.*, **94**: 242–253 (2015).

[49] Regti A., El Kassimi A., Laamari M.R., El Haddad M., Competitive Adsorption and Optimization of Binary Mixture of Textile Dyes: a Factorial Design Analysis, *J. Assoc. Arab Univ. Basic Appl. Sci.*, **24(1)**: 1-9 (2017).

[50] Turabik M., Adsorption of Basic Dyes from Single and Binary Component Systems onto Bentonite: Simultaneous Analysis of Basic Red 46 and Basic Yellow 28 by First Order Derivative Spectrophotometric Analysis Method, *J. Hazard. Mater.*, **158(1)**: 52-64 (2008).

[51] Boumaza S., Kaouah F., Omeiri S., Trari M., Bendjama Z., Removal of Dyes by an Integrated Process Coupling Adsorption and Photocatalysis in Batch Mode, *Res. Chem. Intermed.*, **41(4)**: 2353-2375 (2015).

[52] Boudechiche N., Fares M. , Ouyahiab S. , Yazida H. , Trari M. , Zahra Sadaoui., Comparative Study on Removal of Two Basic Dyes in Aqueous Medium by Adsorption using Activated Carbon from Ziziphus Lotus Stones, *Microchemical Journal.*, **146**: 1010–1018 (2019).

[53] Allen S.J., Gan Q., Matthews R., Johnston P.A., Kinetic Modeling of the Adsorption of Basic Dyes by Kudzu, *Journal of Colloid and Interface Science.*, **286(1)**:101-109 (2005).

[54] Song Y., Hui Xu., Ren J., Adsorption Study for Removal of Sunset Yellow by Ethylenediamine-Modified Peanut Husk, *Desalination and Water Treatment.*,**57(37)**: 1-8(2015).

[55] Demirbas A, Kobya M., Sulak M.T., Adsorption Kinetics of a Basic Dye from Aqueous Solutions onto Apricot Stone Activated Carbon, *Bioresource Technology*.,**99(13)**: 5368–5373 (2008).